

# Spectral and theoretical studies of 2-naphthalenol: an organic nonlinear optical crystalline material

V. CHIȘĂ\*, M. OLTEAN<sup>a</sup>, A. PÎRNĂU<sup>a</sup>, V. MICLĂUȘ<sup>b</sup>, S. FILIP<sup>c</sup>

<sup>a</sup>"Babeș-Bolyai" University, Faculty of Physics, Kogălniceanu 1, RO-400084 Cluj-Napoca, Romania

<sup>b</sup>"Babeș-Bolyai" University, Faculty of Chemistry and Chemical Engineering, Department of Inorganic Chemistry, Arany Janos 11, RO-400028 Cluj-Napoca, Romania

<sup>c</sup>University of Oradea, Faculty of Science, Str. Armatei Romane 5, RO-410087 Oradea, Romania

In this work we will report a joint experimental and theoretical investigation on 2-Naphthalenol, which was shown to be a potential organic non linear optical (NLO) material [1] and has very recently been investigated by single crystal X-ray diffraction method. Our study is aiming to get new insights into molecular structure and properties of this molecule and for this purpose we used FT-IR/ATR and FT-Raman spectroscopies, coupled with quantum chemical calculations performed in the framework of Density Functional Theory (DFT) approach, both for monomer and dimer of 2-Naphthalenol. The hybrid B3LYP exchange-correlation functional was used in conjunction with 6-31 G(d) and cc-pVDZ basis sets for geometry optimization, vibrational and polarizability and hyperpolarizability tensor calculations. Excepting the stretching OH vibration, the remaining experimental vibrational bands are reproduced with a molecular root mean square error of only 14.2 cm<sup>-1</sup> and 14.7 cm<sup>-1</sup> corresponding to the 6-31 G(d) and cc-pVDZ basis sets, respectively. The present calculations with the two different basis sets show the inverse relationship between the first polarizability and the corresponding HOMO-LUMO energy gap. While the dipole moment and polarizability are greater for dimer, the hyperpolarizability is significantly lower and this fact could be ascribed to the minimization of the effect of conjugation length on the second order non linear properties for this molecule.

(Received December 2, 2005; accepted May 18, 2006)

*Keywords:* 2-Naphthalenol, Non-linear optical properties, Vibrational, Density functional theory

## 1. Introduction

Materials with large nonlinear optical properties (NLOP) have recently attracted much interest due to their technological importance in various photonic technologies as: optical communications, optical computing, optical switching and wave-guiding, compact 3D data storage and micro fabrication, chemical and biological sensing, optical power limiting, bio-imaging, signal and data processing, etc. [1-7].

Initially, the research on materials with NLOP properties has been focused on inorganic crystals and semiconductors, but now, organic molecules are increasingly investigated from this perspective [8-17].

The structure of organic NLO materials is based on the  $\pi$ -bond system extended over a large length scale of the molecule, which can be very easily manipulated by substitution of electron donating and electron withdrawing groups around the aromatic moieties, these leading to an increased optical nonlinearity. Apart from structural flexibility, which allows fine-tuning of chemical structures and properties for the desired nonlinear optical properties, the organic materials are of great technological interest because of their low cost, ease of fabrication and integration into devices, low dielectric constant, high electro-optic coefficient, resistance to laser damages.

Polar organic crystals which form non-centrosymmetric crystal structures are attracting much

interest due to their potentially high non-linearities and a rapid response in electro-optic effects that often surpasses those on inorganic non-linear optical materials. Among these, 2N has been recently investigated by X-ray diffraction method and was confirmed that it crystallizes in the monoclinic non-centrosymmetric space group *Ia*. This fact supports the assumption that 2N crystals may be considered as potential organic NLO material.

## 2. Experimental

2-Naphthalenol was purchased from a commercial source and used without further purification. FT-IR/ATR spectra for 2N powder sample were recorded at room temperature on a conventional Equinox 55 FT-IR spectrometer equipped with an InGaAs detector, coupled with a Bruker Miracle ATR sampling device. The FT-Raman spectra were recorded in a backscattering geometry with a Bruker FRA 106/S Raman accessory attached to the FT-IR spectrometer. The 1064 nm Nd:YAG laser was used as excitation source and the laser power was set to 400 mW. All spectra were recorded with a resolution of 4 cm<sup>-1</sup> by co-adding 32 scans.

### 2.1 Computational details

The molecular geometry optimizations and vibrational frequencies calculations were performed with the Gaussian

98 W software package [18] by using DFT approach, with the hybrid functional obtained by combining the Becke's three parameter exchange functional [19] with the correlation functional proposed by Lee, Yang and Parr. The split-valence 6-31G(d) basis set of the Pople's group [20] and the correlation consistent basis set cc-pVDZ have been used for the expansion of molecular orbitals. All the calculations have been carried out with the restricted closed-shell formalism. The geometries were fully optimized without any constraint with the help of analytical gradient procedure implemented within Gaussian 98W program. The force constants were calculated by analytical differentiation algorithms, for each completely optimized geometry. Prior to compare the calculated vibrational frequencies with the experimental counterparts the former have been scaled by appropriate scaling factors recommended by Scot and Radom [21] and by Sinha et al. [22] for the 6-31G(d) and cc-pVDZ basis sets, respectively.

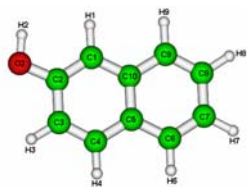
### 3. Results and discussion

#### 3.1 Vibrational frequencies

Vibrational spectra (FT-IR/ATR and Raman) of 2-Naphthalenol are given in Fig.1 and in Table 1 are summarized the experimental and calculated normal modes. The last column contains the motions that contribute the most to the different normal modes, according to B3LYP/6-31G(d) calculations.

In Fig. 2 is given the correlation diagram between the experimental and calculated vibrational frequencies of 2-Naphthalenol molecule. The computed vibrational wave-numbers reported in Table 1 are scaled with 0.9614 scaling factor [21].

Excepting the  $\nu(\text{OH})$  vibration, the mean absolute deviation and the molecular root mean square error (rms) in reproducing the remaining experimental vibrational bands of 2N with the basis set 6-31G(d) (cc-pVDZ) are  $9.4 \text{ cm}^{-1}$  ( $10.3 \text{ cm}^{-1}$ ) and  $14.2 \text{ cm}^{-1}$  ( $14.7 \text{ cm}^{-1}$ ), respectively. The maximum absolute deviation between the experimental and computed data for the two basis sets are  $46 \text{ cm}^{-1}$  and  $44.0 \text{ cm}^{-1}$  and in both cases they correspond to the  $\gamma(\text{OH})$  vibration. It is well known that free OH group has characteristic stretching vibration close to  $3600 \text{ cm}^{-1}$  [23]. This value is nicely reproduced in our case after an appropriate scaling and the large red shift of this frequency in the experimental vibrational spectra of 2N and thus the large discrepancy between the calculated and experimental  $\nu(\text{OH})$  frequency can be explained by intermolecular interactions [24].



B3LYP/6-31G(d) optimized molecular structure and atom numbering scheme for 2-Naphthalenol.

Indeed, X-ray data [1] show that in solid phase, each 2N molecule is linked to two neighboring non-equivalent molecules through OH...O intermolecular hydrogen bonds with donor-acceptor distances of  $2.764 \text{ \AA}$  and  $2.752 \text{ \AA}$ , respectively. Similar deviations  $\nu(\text{OH})$  wave-number have been observed for related  $\pi$ -conjugated molecules like naphthazarin [25].

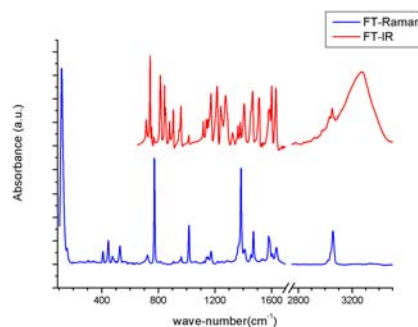


Fig. 1. FT-IR/ATR (top) and Raman (bottom) spectra of 2-Naphthalenol.

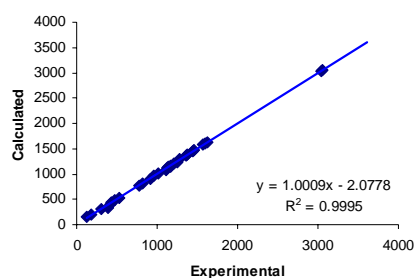


Fig. 2. Correlation diagram for experimental vs. computed vibrational frequencies of 2-Naphthalenol at B3LYP/6-31G(d) level of theory.

As seen in Table 1, in plane bending OH vibration is distributed over a number of normal modes, preserving however a very good match between the experimental and computed frequencies. According to calculations, out of plane OH bending is predicted at  $386 \text{ cm}^{-1}$ , significantly higher than the experimental value of  $340 \text{ cm}^{-1}$ .

Ring stretchings vibrations are coupled with in plane CH or OH bendings and are very well reproduced by B3LYP/6-31G(d) theoretical method. Even the usually anharmonic CH stretchings are very well predicted by DFT method, with a uniform frequency scaling procedure. Among the out of plane CH bending vibrations, only the band calculated at  $1106 \text{ cm}^{-1}$  differ significantly from the experimental counterparts. The most intense band in the FT-IR/ATR spectrum is due to the  $\gamma(\text{CH})$  vibration which is again in good agreement with experiment. In the Raman spectrum, the most intense bands ( $1383$  and  $772 \text{ cm}^{-1}$ ) have a dominant  $\nu(\text{CC})$  and ring breathing character, respectively.

As seen in Fig. 2, there is a very good correlation between the experimental and calculated wave-numbers of 2-Naphthalenol which allow us to confidently assign the vibrational spectrum of this molecule.

Table 1. Selected experimental and theoretical (B3LYP/6-31G(d)) vibrational bands of 2-Naphthalenol.

Mode	Experimental		Calculated	Assignments*
	FT-IR/ATR	Raman		
1	3268		3605	v(OH)
2	3082		3085	v(CH)
3	3067		3064	v(CH)
4	3053	3057	3054	v(CH)
5	3033	3040	3040	v(CH)
6	1629	1632	1625	v(CC)+δ(CH)
7	1601	1603	1601	v(CC)+δ(CH)
8	1584	1586	1573	v(CC)+δ(OH)+δ(CH)
9	1512		1517	v(CC)+δ(OH)+δ(CH)
10	1465	1472	1465	v(CC)+δ(CH)+δ(OH)
11	1453	1453	1446	v(CC)+δ(CH)+δ(OH)
12	1379	1383	1376	v(CC)+δ(CH)+δ(OH)
13	1363	1365	1365	d(CCC)+v(CC)+δ(CH)+δ(OH)
14	1324		1355	v(CC)+δ(CH)+δ(OH)
15	1287	1287	1278	v(CO)+δ(CCC)+δ(OH)+δ(CH)
16	1240	1239	1247	δ(CCC)+δ(CH)+δ(OH)
17	1215	1218	1213	δ(CH)+δ(OH)+d(CCC)
18	1172	1171	1172	δ(OH)+δ(CH)+v(CO)+v(CC)
19	1149	1148	1164	δ(OH)+δ(CH)
20	1138	1138	1139	δ(OH)+δ(CH)
21	1118	1121	1130	δ(CH)+δ(OH)
22		1067	1106	δ(CH)+δ(CCC)
23	1014	1015	1011	d(CCC)+δ(CH)
24	959	959	965	γ(CH)
25	946		948	γ(CH)+γ(CC)
26	905	905	917	δ(CCC)+δ(CH)
27	878		883	γ(CH)+γ(CC)
28	843		843	γ(CH)
29	813	813	825	γ(CH)+γ(CC)
30	775	772	784	ring breathing
31	769		767	γ(CC)+γ(CH)+γ(CO)
32	740		762	γ(CH)
33	714		729	δ(CCC)
34		527	531	δ(CCC)
35		475	468	δ(COH)+δ(CCC)
36		444	429	δ(COH)+δ(CCC)
37		406	410	γ(CC)+γ(CH)+γ(OH)+γ(CO)
38		340	386	γ(OH)
39		303	303	γ(COH)+τ(rings)
40		203	185	τ(rings)
41		155	125	τ(rings)

\* v-stretching, δ-in plane bending, γ-out-of-plane bending, τ-twisting

### 3.2. Polarizability and hyperpolarizability

Quantum chemical methods are an invaluable and inexpensive tool for predicting the molecular NLO

properties of different molecules by analyzing their potential before synthesis.

We calculated the electric dipole moments ( $\mu$ ), polarizability ( $\langle\alpha\rangle$ ) and hyperpolarizability ( $\beta$ ) of 2-Naphthalenol with the hydroxyl group as donor substituent. After the energy of the molecular system is obtained, the static response properties electric dipole moment, polarizability and hyperpolarizability of a molecular system are then calculated as the derivatives of the energy with respect to the electric field components, taken at zero field:

dipole moment:

$$\mu_i = -\left(\frac{\partial E}{\partial F_i}\right)_0$$

components of polarizability tensor:

$$\alpha_{ij} = -\left(\frac{\partial^2 E}{\partial F_i \partial F_j}\right)_0$$

components of the first hyperpolarizability tensor:

$$\beta_{ijk} = -\left(\frac{\partial^3 E}{\partial F_i \partial F_j \partial F_k}\right)_0$$

The static electric polarizability  $\alpha$  express the capacity of the charge density of a system to be distorted by an external electric field. Usually, only the average value of its diagonal elements is given:

$$\langle\alpha\rangle = \frac{1}{3}(\alpha_{xx} + \alpha_{yy} + \alpha_{zz})$$

The total first static hyperpolarizability is obtained from the equation:

$$\beta_{tot} = (\beta_x^2 + \beta_y^2 + \beta_z^2)^{1/2}$$

upon calculating the individual static components:

$$\beta_i = \beta_{iii} + \frac{1}{3} \sum_{i \neq j} (\beta_{ijj} + \beta_{jjj} + \beta_{jji})$$

Due to the Kleinman symmetry [26] ( $\beta_{xyy} = \beta_{yyx} = \beta_{yxy}, \dots$ ) one finally obtains the equation for the total first hyperpolarizability:

$$\beta_{tot} = [(\beta_{xxx} + \beta_{xyy} + \beta_{xzz})^2 + (\beta_{yyy} + \beta_{yzz} + \beta_{yxx})^2 + (\beta_{zzz} + \beta_{zxx} + \beta_{zyy})^2]^{1/2}$$

The electric dipole moment, polarizability and hyperpolarizability tensors have been calculated in finite field (FF) approach and they are given in Tables 2-4, respectively. The calculations have been performed on monomer and dimer of 2N by using the hybrid B3LYP functional, in conjunction with 6-31G(d) and correlation consistent cc-pVDZ basis sets.

Table 2. B3LYP calculated total electric dipole moment (Debye) for 2-Naphthalenol.

	monomer	dimer
6-31G(d)	1.093	3.581
cc-pVDZ	1.067	3.575

The contraction schemes for cc-pVDZ and 6-31G(d) basis sets are [27] (9s,4p,1d/4s,1p)  $\rightarrow$  [3s,2p,1d/2s,1p] and (10s,4p,1d/4s)  $\rightarrow$  [3s,2p,1d/2s], respectively. The former basis set includes by definition polarization functions on hydrogen atoms, while the latter includes polarization functions only for heavy atoms (C, N and O atoms). Moreover, for cc-pVDZ, the core 1s and 2s orbitals for heavy atoms are described by contractions consisting of 8 GTO. As seen in these tables, the polarization functions on hydrogen atoms do not influence in a significant manner the dipole moment, polarizability or first hyperpolarizability tensors.

Table 3. B3LYP calculated diagonal elements for the polarizability tensor of 2-Naphthalenol (a.u.).

	$\alpha_{xx}$	$\alpha_{yy}$	$\alpha_{zz}$	$\langle\alpha\rangle$
<b>monomer</b>				
6-31G(d)	164.929	114.955	34.531	104.805
cc-pVDZ	171.020	120.472	39.110	110.201
<b>dimer</b>				
6-31G(d)	270.633	226.587	151.106	216.109
cc-pVDZ	287.891	238.981	155.912	227.595

The trends (increase in  $\langle\alpha\rangle$  and  $\beta$ ) observed with the "spectroscopic" 6-31G(d) basis set are preserved with the cc-pVDZ, both for monomer and dimer of 2-Naphthalenol. According to calculations, the medium polarizability for dimer is significantly higher than for monomer. This could be related to the HOMO-LUMO gap which is calculated for the two systems. As shown in Table 5, while the HOMO energy is increasing when passing from monomer to dimer, the LUMO's energy is lowering roughly with the same energy, resulting in a smaller HOMO-LUMO gap for the two systems. Minor differences are noted between the two basis sets in the predicted energies related to the frontier orbitals.

Table 4. B3LYP calculated components and total values for the first hyperpolarizability tensor of 2-Naphthalenol ( $10^{-30}$  esu).

	$\beta_{xxx}$	$\beta_{xyy}$	$\beta_{yzz}$	$\beta_{yyv}$	$\beta_{vzz}$	$\beta_{vxx}$	$\beta_{zzz}$	$\beta_{zxx}$	$\beta_{zyy}$	$\beta_{tot}$
<b>monomer</b>										
6-31G(d)	351.557	-3.937	0.009	0.026	0.240	66.231	-0.001	-14.926	-0.583	354.272
cc-pVDZ	381.275	-1.148	0.008	0.008	0.602	69.510	0.001	-14.953	3.984	386.704
<b>dimer</b>										
6-31G(d)	-95.041	21.533	74.905	12.126	-4.008	-52.303	-83.368	33.007	-75.622	133.513
cc-pVDZ	-84.479	18.775	90.585	12.345	6.312	-15.833	-91.170	16.421	-61.616	138.644

Table 5. B3LYP calculated energies (eV) of the frontier orbitals for 2-Naphthalenol.

	system	6-31G(d)	cc-pVDZ
HOMO	monomer	-5.58	-5.73
	dimer	-5.29	-5.47
LUMO	monomer	-0.90	-1.11
	dimer	-1.17	-1.40
$\Delta E$	monomer	4.69	4.62
	dimer	4.12	4.07

The first static hyperpolarizability is also significantly affected by the basis set used in calculations and again the cc-pVDZ basis set gives larger  $\beta$  values than the standard one. In addition,  $\beta$  values are drastically lowered in the case of dimer so it is clear that  $\beta$  does not follow the same trend as  $\alpha$  does, with the HOMO-LUMO gap. This behavior could be explained by a poor communication between the two frontier orbitals of dimer (see Fig. 3) which are located on the two different aromatic rings of the molecule. This could lead to a minimization of the effect of the conjugation length on the second order non linear optical properties and hence significantly reduced  $\beta$  values are expected.

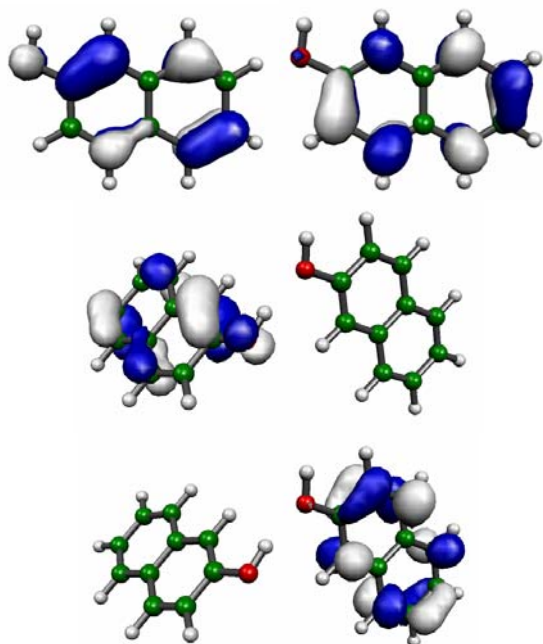


Fig. 3. Representation of the HOMO (left) and LUMO (right) orbitals of 2-Naphthalenol monomer (top) and dimer (bottom).

#### 4. Conclusions

The very good correlation between the experimental and calculated wave-numbers of 2-Naphthalenol allow us to confidently assign the vibrational spectrum of this molecule. The only significant discrepancy between experiment and theory is noted for the broad band centered at  $3268\text{ cm}^{-1}$ . However, this band can easily be assigned to the  $\nu(\text{OH})$  vibration with the hydroxyl group involved in intermolecular interactions.

Rather great hyperpolarizability derived by theoretical calculations at B3LYP/6-31G(d) level of theory suggests the possible future use of this compound for electro-optics applications.

The poor communication between the frontier orbitals of 2-Naphthalenol dimer could lead to a minimization of the effect of the conjugation length on the second order non linear optical properties with significantly reduced  $\beta$  values.

#### References

- [1] B. Marciniak, E. Rozyca-Sokolowska, V. Pavlyuk, *Acta. Cryst.*, **E59**, o52 (2003).
- [2] A. Datta, S. K. Pati, *J. Phys. Chem. A*, **108**, 320 (2004).
- [3] H. Unver, A. Karakas, A. Elmali, T. N. Durlu, *J. Mol. Struct.* **737**, 131 (2005).
- [4] A. Karakas, A. Elmali, H. Unver, I. Svoboda, *J. Mol. Struct.* **702**, 103 (2004).
- [5] K. S. Thanthiriwatte, K. M. Nalin de Silva, *J. Mol. Struct. (Theochem)* **617**, 169 (2002).
- [6] P. J. Mendes, J. P. Prates Ramalho, A. J. E. Candeias, M. P. Robalo, M. H. Garcia, *J. Mol. Struct. (Theochem)* **729**, 109 (2005).
- [7] J. Zyss, *Molecular Nonlinear Optics*, Academic Press, Boston, 1994.
- [8] E. E. Moore, D. Yaron, *J. Phys. Chem. A* **106**, 5339 (2002).
- [9] B. H. Cumpston et al., *Nature* **398**, 51 (1999).
- [10] S. Kawata, Y. Kawata, *Chem. Rev.* **100**, 1777 (2000).
- [11] N. Dietz, F. L. Madarasz, *Mat. Sci. Eng. B* **97**, 182 (2003).
- [12] T. Pons, L. Moreaux, O. Mongin, M. Blanchard-Desce, J. Mertz, *J. Biomed. Opt.* **8**, 428 (2003).
- [13] M. G. Silly, L. Porres, O. Mongin, P. A. Chollet, M. Blanchard-Desce, *Chem. Phys. Lett.* **379**, 74 (2003).
- [14] C. Bauer, B. Schnabel, E. B. Kley, U. Scherf, H. Giessen, R. F. Mahrt, *Adv. Mat.* **14**, 673 (2002).
- [15] W. R. Zipfel, R. M. Williams, R. Christie, A. Y. Nikitin, B. T. Hyman, W. W. Webb, *Proc. Natl. Acad. Sci. USA* **100**, 7075 (2003).
- [16] M. Drozd, M. K. Marchewka, *J. Mol. Struct. (Theochem)*, **716**, 175 (2005).
- [17] S. Dhanuskodi, S. Manikandan, *Cryst. Res. Technol.* **39**, 586 (2004).
- [18] *Gaussian 98, Revision A.7*, M. J. Frisch, G. W. Trucks, H. B. Schlegel, G. E. Scuseria, M. A. Robb, J. R. Cheeseman, V. G. Zakrzewski, J. A. Montgomery, Jr., R. E. Stratmann, J. C. Burant, S. Dapprich, J. M. Millam, A. D. Daniels, K. N. Kudin, M. C. Strain, O. Farkas, J. Tomasi, V. Barone, M. Cossi, R. Cammi, B. Mennucci, C. Pomelli, C. Adamo, S. Clifford, J. Ochterski, G. A. Petersson, P. Y. Ayala, Q. Cui, K. Morokuma, D. K. Malick, A. D. Rabuck, K. Raghavachari, J. B. Foresman, J. Cioslowski, J. V. Ortiz, A. G. Baboul, B. B. Stefanov, G. Liu, A. Liashenko, P. Piskorz, I. Komaromi, R. Gomperts, R. L. Martin, D. J. Fox, T. Keith, M. A. Al-Laham, C. Y. Peng, A. Nanayakkara, C. Gonzalez, M. Challacombe, P. M. W. Gill, B. Johnson, W. Chen, M. W. Wong, J. L. Andres, C. Gonzalez, M. Head-Gordon, E. S. Replogle, J. A. Pople, Gaussian, Inc., Pittsburgh PA, (1998).
- [19] A. D. Becke, *J. Chem. Phys.* **98**, 5648 (1993); A. D. Becke, *Phys. Rev.* **38**, 3098 (1998); C. Lee, W. Yang, R. G. Parr, *Phys. Rev. B* **37**, 785 (1988).
- [20] W. J. Hehre, L. Radom, P. V. R. Schleyer, J. A. Pople, "Ab Initio" Molecular Orbital Theory, John Wiley & Sons, New York, 1986.
- [21] A. P. Scott, L. Radom, *J. Phys. Chem.* **100**, 16502 (1996).
- [22] P. Sinha, S. E. Boesch, C. Gu, R. A. Wheeler, A. K. Wilson, *J. Phys. Chem. A*, **108**, 9213 (2004).
- [23] H. G. Korth, M. I. de Heer, P. Mulder, *J. Phys. Chem.* **106**, 8779 (2002).
- [24] K. Muller-Dethlefs, P. Hobza, *Chem. Rev.* **100**, 143 (2000).
- [25] M. Z. Tabrizi, S. F. Tayyari, F. Tayyari, M. Behforouz, *Spectrochim. Acta A*, **60**, 111 (2004).
- [26] D. A. Kleinman, *Phys. Rev.* **126**, 1977 (1962).
- [27] F. Jensen, *Introduction to Computational Chemistry*, John Wiley and Sons, 1999, p.162.

\* Corresponding author: vchis@phys.ubbcluj.ro